I2SM

International Symposium on Sediment Management

Lille, July 9-11th, 2008

Edited by : N-E. ABRIAK
D. DAMIDOT
R. ZENTAR

Understanding Sedimentary Processes and degree of pollution through Geochemistry and magnetic properties of mudflat sediments from a Tropical microtidal estuary, Central West Coast of India.

Ksh. Tomchou Singh1, G. N. Nayak1*, D. V. Borole2, N. Basavaiah3

1Dept. of Marine Science, Goa University, Goa, India.
Email - tomchou_kshetri@yahoo.com
**Email- nayak1006@rediffmail.com*
gnnayak@unigoa.ac.in
2National Institute of Oceanography, Dona Paula, Goa, India. Email-dnyan@nio.org.
3Indian Institute of Geomagnetism, New Panvel, Navi Mumbai, India. Email-bas@iigs.iigm.res.in

Abstract: Two shallow cores (Core GN and GH) collected from two tidal mudflats in the Aghanashini or Tadri River Estuary were analyzed for sediment components viz sand, silt, clay and Organic Carbon (OC); geochemistry and magnetic properties to assess the variations in distribution, sedimentary processes and historical pollution records. The core GH is of mature mudflat consisted of slightly sandy mud with higher concentrations of Ca, Mg and Mn together with higher silt, clay and OC percentage, which is likely because of more marine influences in this mudflat and by grain size effect whereas core GN is characterized by comparatively coarser sediments of sandy mud of a mudflat environment and shows higher concentrations of Pb and Co together with higher value of sand, which are likely to be caused by comparatively nearer to continental source reflecting a pollution origin. The unsupported ^{210}Pb activity in core GH exhibit enhanced sedimentation rates for last 13 years, which is likely to be a response to the human impact in the form of differential erosion and accelerated sedimentation in combination with relative sea level rise. The geochemical data indicates that both Mn and Fe have been remobilized and that these diagenetic processes have slightly modified the vertical distributions of Zn, Cu, Cr and Co. The magnetic data reveal evidence for changes in magnetic mineralogy and grain size within the cores. In both the cores, there is substantial decrease in total magnetic concentration and coarsening of the magnetic grain size, but at different depths, which is in agreement with Fe and Mn profiles, suggesting dissolution of fine grained magnetite under reducing conditions. However, general trends in pollutant loading, as indicated by EF of Cu, Cr, Co and Fe can still be identified in Core GH with maximum inputs (EF > 1.5) occurring around 1900 increasing towards the present day. Both cores show closely similar traces of gradual increase of hematite and magnetite deposition with a steeper rise of hematite in the upper part of the respective cores which may reflect the increased erosion of more weathered (magnetically harder) materials with increase in anthropogenic activities. Though, the construction of pollution chronology in the core GN is limited by different processes, unlike in core GH, Pb shows gradually increasing trend towards the surface with enrichment values above 5 which may signify input of higher degree of contamination upstream side of the estuary.

Keywords: mudflats; pollution; diagenetic processes; cores; Tadri Estuary.

Introduction

Sediments constitute the main component in estuarine mudflats and the study of the spatial and temporal distribution of sediment components, metals and sedimentation pattern would provide fundamental information for understanding a wide variety of environmental issues. The estuarine mudflats are predominantly areas of deposition and important reservoirs for contaminants as they tend to act as sink for fine, contaminant-reactive sediments, and historically, have acted as centers

for industrial and urban development. Industrial and urban expansion around estuaries has commonly led to an increased input of heavy metals, a fraction of which sorb on to fine-grained suspended material and are subsequently deposited and buried in sub and intertidal mudflats. So, analysis of cores of undisturbed sediment from their sub environments may allow reconstructing recent and historical inputs of metal contaminants. Records of environmental change are often preserved in sediment from subtidal and intertidal mudflats and salt marshes. A study of these sediments allows an assessment to be made of the scale of pollutant inputs from past industrial and urban development [1, 2, 3]. However, establishing a reliable chronology depends upon whether or not there has been significant early diagenetic remobilization of either the contaminants or the radionuclides used for dating. In Indian context, there is still paucity of information about these highly sensitive and important areas of interface between land and sea. As witnessed from available literature, less works has been carried out in the estuarine tidal mudflats especially along west coast of India. However, mudflats are coming under increasing stress from human activity and the global climate change. There is increasing concern over the effects of anthropogenic inputs with the increase in population and associated rapid industrialization in and around the coast of India. In summary, the estuarine mudflats are very sensitive to both manmade as well as natural environmental changes and preserve the characteristic changes that can be studied through sediments deposited with time. Through the present study, an attempt has been made to understand the processes affecting the distribution of sediment components and the abundance of heavy metals, which will reflect the environmental status of recent past.

Study area

The Aghanashini or Tadri Estuary in Karnataka, is one of the estuaries along the West Coast of India (Fig. 1).The Aghanashini or Tadri is about 121km long and falls in to the Arabian Sea about 10 km south of the Gangavali River.

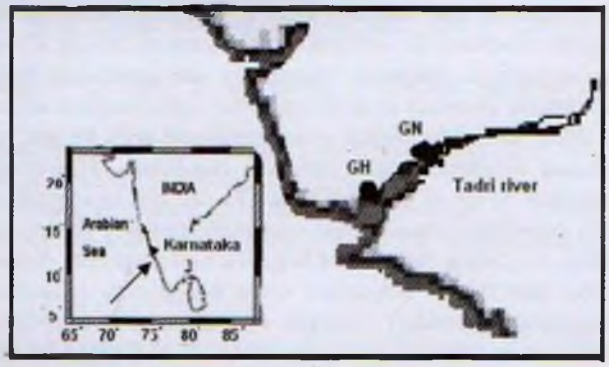

Fig. 1. Study area with core locations

It has two sources, the Bakurhole rising in a pond at Manjuguni about 25 km west of Sirsi and the Donihalla whose source is close to Sirsi. At Uppnapattana, the Donihalla meets the tide. Further the remaining portion of the river (24 km) downstream is navigable to craft of four to nine tones is known as either the Tadri or as the Aghanashini River. The outlet to the sea is between two hills. The area is characterized by high humidity, nearly all the year round in the coastal strip and in the Western Ghats region, while in the area to the east of the Ghats, the climate is drier, except in the south west monsoon season. The average annual rainfall is 3500 mm. Geologically, the area consists of rock formation of Archean complex which are divided into an older group of Dharwar system and a younger group termed as Peninsular Gneisses. Both the Dharwar and the Peninsular Gneisses are frequently overlain by a capping of laterite which is the source of iron and manganese ores.

Methodology

Two shallow cores (< 1m), one (Core GN) from interior of the estuary and other (Core GH) relatively nearer to the mouth, were collected from two tidal mudflats in the Aghanashini or Tadri River Estuary (Fig. 1) using hand driven PVC coring tube. Cores were then sub-sampled with 2 cm interval with a plastic spatula to avoid the metal contamination, which were then transferred to cleaned polyethylene bag and stored in icebox till it reached the laboratory. On return to the laboratory sediments were dried at 60 degree overnight and kept ready for analysis. Sand, silt and clay analysis was carried out by wet sieving and pipette method following Folk [4]. Organic carbon estimation was carried out by wet oxidation methods of Gaudette et al. [5] in which exothermic heating and oxidation with $K_2Cr_2O_7$ and concentrated H_2SO_4 are followed by titration of excess dichromate with 0.5 N Fe $(NH_4)_2(SO4)_2.6H_2O$. Sediment samples for major and trace metal analysis were digested by using hydrofluoric – perchloric – nitric acid mixtures in Teflon beakers. Complete digestion was ensured repeating the digestion steps until the clear solutions were obtained. The resulted solutions were analyzed for Al, K, Ca, Mg, Fe, Mn, Zn, Cu, Cr and Co by Atomic Absorption Spectrophotometer (GBC 932 AA). Precision was monitored by analyzing triplicate samples for some selected samples and was generally < 6 % standard deviation (%SD) for major and trace elements. Accuracy of the method was determined by comparing with reported values of certified standard (GSJ-JSd-1) and was ±3% for Zn; ±6% for Fe and ±10 %for Mn, Al, Ca, Mg and K, and ±15 % for Cu and Pb of the working values quoted. X – ray diffraction studies were carried out on a Philips X – ray diffractometer. Relative percentages of different clay minerals were estimated by weighing the integrated peak areas of basal reflections in the glycolated X-ray diffractograms, following the semi quantitative method of Biscaye [6]. The samples of Cores MS, MR and ZA were subjected to ^{210}Pb dating by Alpha Spectrometer to estimate sediment accumulation rate. The ^{210}Pb was measured via its daughter nuclide ^{210}Po, using the standard radiochemical procedure of Flynn (1968). Magnetic susceptibility analysis was performed on bulk samples using Bartington MS2 magnetic susceptibility meter and KLY – 2 Kappabridge (Agico). Anhysteretic remanent magnetization (ARM) with peak alternating field of 100 mT and decreasing amplitude was imposed on a steady field of 0.1mT, and the remanence was measured with a Molspin spinner pulse magnetometer. Isothermal remanent magnetization (IRM) was measured using a Molspin spinner pulse magnetometer after each step in a sequence of reverse field DC demagnetization stages at -20 mT, -30 mT, -40 mT, -100 mT, -200 mT and -300 mT. The IRM acquired at 2T is referred to as the saturation isothermal remanent magnetization (SIRM). The results were then used to calculate mass-specific magnetic parameters and inter-parameter ratios. To quantify the absolute concentration of high coercivity components 'Hard' IRM (=SIRM+ $IRM_{.300mT}$) and 'Soft' IRM (= SIRM – $IRM_{.20mT}$) parameters [7] and S-ratio (=$IRM_{.300mT}$/ SIRM) [8] were evaluated. Isocon diagram of Grant [9] has been used to show how concentrations are varying between the different cores. To evaluate anthropogenic influences of heavy metals in sediments, enrichment factor (EF) was used as an index, which is the observed metal to aluminum ratio in the sample of interest divided by the background metal/aluminum ratio. It is expressed mathematically as

$$EF = (Me/Al)_{Sample} / (Me/Al)_{Background}$$

Where $(Me/Al)_{Sample}$ is the metal to Al ratio in the samples of interest, $(Me/Al)_{Background}$ is the natural background value of metal to Al ratio [10].

The geochemical data of the Post Archean Average Shale (PAAS) given by Turekian and Weedchpohl [11]was used as the background.

Results and discussion

Sediment components (sand, silt, clay and organic carbon)

In core GH, the sand, silt and clay data obtained show a range of 3.04 - 19.92%; 28.20 - 57.19% and 29.68 - 60.32% respectively and the sediment is muddy with an average value of 89.28% of silt and clay out of which clay (avg.47.32%) is dominated to silt (avg. 41.96%). The sand profile (Fig. 2A) shows an increasing trend from the base of the core up to 52 cm depth with a plateau at 60 to 66 cm and then a gradually decreasing trend towards the surface. Silt shows nearly constant trend with some ups and downs whereas clay shows an opposite distribution to sand with a decreasing trend from base to 52 cm depth from where it increases till the surface of the core. So the core can be divided into two distinct zones marked by variations of sand and clay as lower 66 – 52 cm where the decrease in clay is compensated by the increase in sand and an upper 52 – 0 cm zone where sand decreases in the expense of clay. Organic carbon value ranges from 1.26 to 4.92% with an average value of 3.08%. The profile of organic carbon also shows two distinct zones with a nearly constant trend in the lower 66 – 52 cm portion then it suddenly increases up to 50 cm and then shows decreasing trend in the upper 50 – 0 cm portion. The organic carbon profile agrees with the sand profile except at top 8 cm where it agrees with clay.

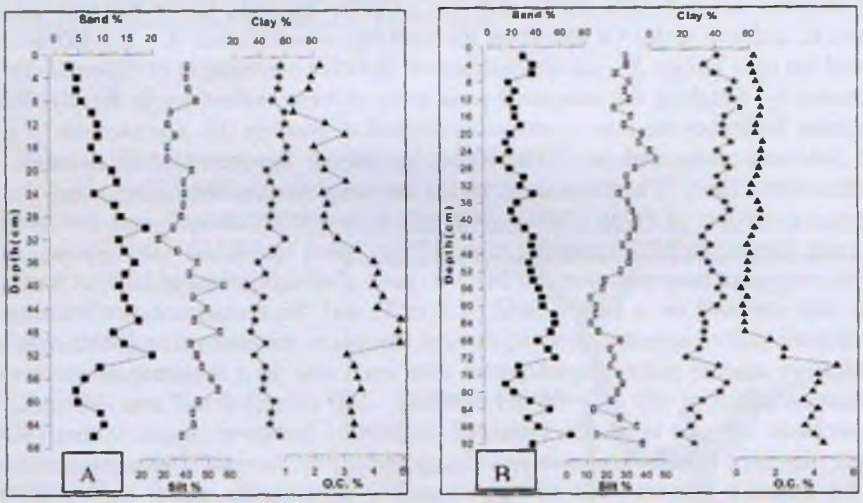

Fig.2. Down core variation of sediment components: A – core GH, B – core GN.

In core GN, the data show a range of 9.00 to 67.38% sand, 11.95 to 45.50% silt and 17.40 to 54.13% clay and the clay is the dominating component with an average value of 38.24% followed by sand and silt with average values of 32.15% and 27.71% respectively. Sand and silt profiles (Fig. 2B) with depth show an opposite distribution with three distinct portions, while clay shows a nearly decreasing trend with depth. In the bottom 92 – 64 cm portion sand decreases which is compensated by increase in silt. In the middle 64 - 26 cm portion, sand decreases in the expense of silt while the increase in sand is compensated by the decrease in clay in the top 26 – 0 cm portion. The organic carbon value ranges from a minimum of 0.25% to a maximum of 4.47% with an average value of 1.68%. The organic carbon profile shows a nearly constant trend of relatively high values from the base of the core to 74 cm from where values suddenly decrease up to 66 cm depth and then maintains a gradually increasing trend towards the surface. The distribution of organic carbon largely agrees with clay in the upper portion.

The organic carbon content in core GH shows good correlation with sand (r = 0.50) and silt (r = 0.53) but very poor association with clay (r = - 0.73). So, individually distribution of organic carbon is controlled by sand and silt. In core GN, organic carbon content showed no association with any of the sediment fraction (0.01, sand; - 0.05, silt and -0.37, clay). The gradual increase in organic carbon towards the surface can be seen in the upper portion of the core GN and to some extent in the top most portion of core GH, which are generally attributed to degradation, and such profiles are frequently observed in sandy marine sediments. Although some degradation of organic matter must be occurring in the sediments, the dominant control on organic matter content in core GH seems to be due to the proportion of sand- silt particles.

Further, the changes in sediment characters within the cores are analyzed by plotting the sediment data in ternary diagram proposed by Reineck and Siefert [12]. According to this diagram (Fig. 3A), core GH falls in mature mudflat class throughout the core while core GN changes from mudflat to mixedflat and from mixedflat to mudflat with time.

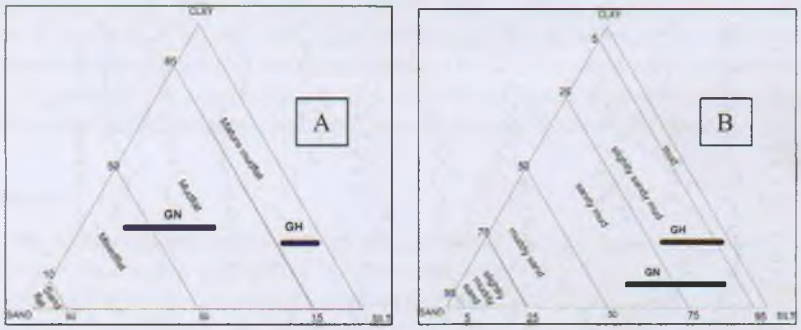

Fig. 3. Ternary diagrams for the textural classification of sediments on the basis of sand/mud ratios. A: after Reineck and Siefert (1980). B: Flemming (2000).

Similarly, variation in grain size characters is also witnessed when the data is plotted in ternary diagram (Fig. 3B) of Flemming [13]. It is found that sediments of core GH have undergone change from slightly sandy mud to mud with time while in core GN sediments are graded from sandy mud to slightly sandy mud again from slightly sandy mud to sandy mud with time. Therefore, it is clear that core GN shows high variations in sediment characters with repetitions of classes in between while core GH is showing gradually fining of sediments with time. Further an attempt has been made to infer the hydrodynamic condition of the depositional environment by using the ternary diagram (Fig. 3C) developed by Pejrup [14]. In the present study, the components plotted for core GH, largely fall in group II (B and C), which represents a relatively quiet hydrodynamic condition. On the other hand, core GN falls under group II (C and D) and III (C and D), which represents the relatively violent hydrodynamic conditions.

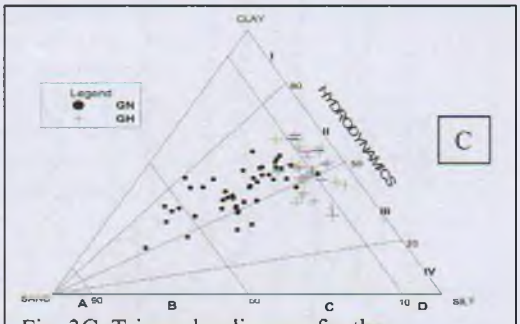

Fig. 3C. Triangular diagram for the classification of hydrodynamic conditions after Pejrup (1988).

Geochemistry

Major element profiles, in core GH, do not agree with any of the sediment component profiles (Fig. 4A). Al profile shows three portions of distinct distribution with bottom portion 66 – 54 cm of high value but decreasing trend which is followed by middle 54 - 18 cm of constant trend while a low value but highly fluctuating trend characterized the top 18 – 0 cm upward. K shows a nearly constant trend throughout the core while Mg shows an erratic trend in the bottom portion of 66 – 48 cm and then a decreasing trend of ups and downs up to 34 cm before it maintains an increasing trend towards the surface. Ca shows an enriched bottom portion of 66 – 46 cm with spikes of high values in between and almost a constant trend in the top 46 - 0 cm towards the surface. In case of core GN, Al, Mg and K profiles agree with silt profile and to some extent with clay profile (Fig.4B). All these elements show three distinct portions with an enriched but decreasing bottom portion of 92 – 64 cm followed by middle portion 64 – 28 cm of increasing trend and then decreasing trend towards the surface. Ca shows a constant trend from the base of the core up to 68 cm from where values increase suddenly before maintaining a more or less increasing trend towards the surface.

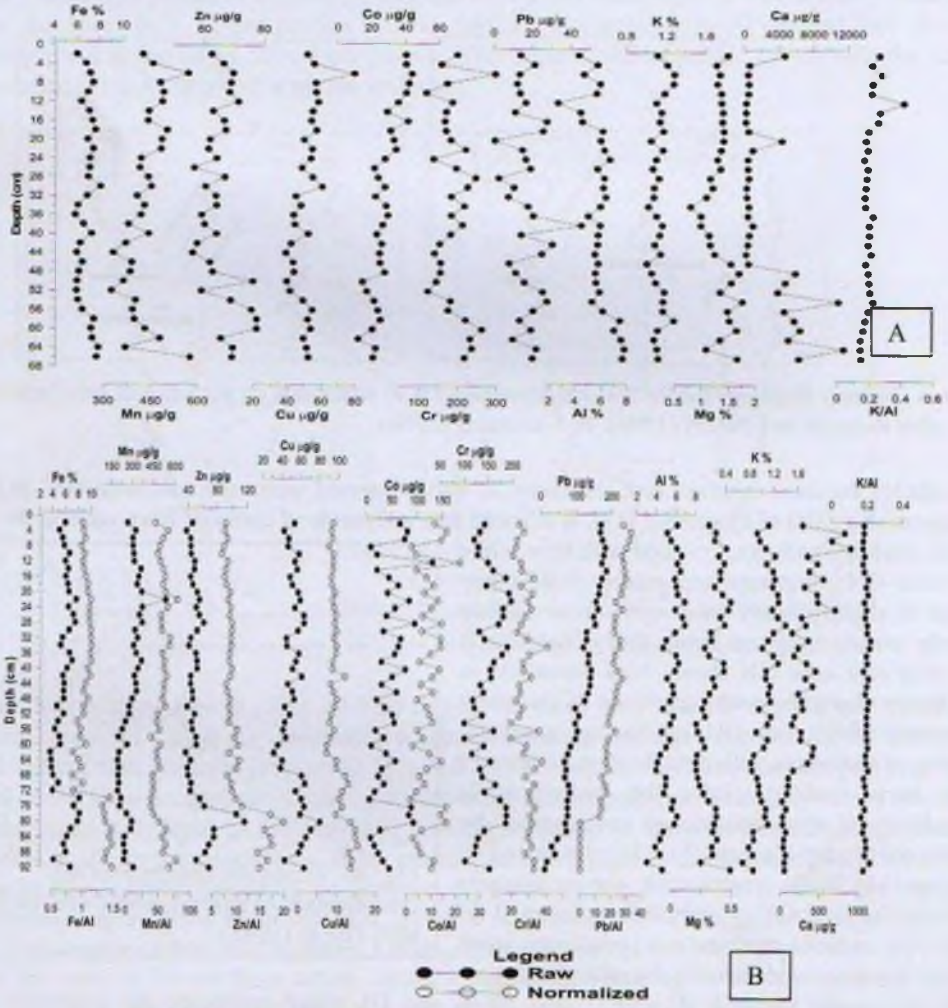

Fig. 4 Down core variation of metals: A – core GH, B – core GN.

In both the cores, almost all the heavy metals including Fe and Mn show broad similarities in distribution with depth. In core GH, geochemical data shows a range of 6.03 – 7.92 % Fe, 362 - 574.75 µg/g Mn, 56.25 - 77.78 µg/g Zn, 41.50 - 79.00 µg/g Cu, 118.00 - 295.00 µg/g Cr, 12.50 - 43.75 µg/g Co and 0.75 - 30.75 µg/g for Pb. All the metals except Co and Pb show three distinct portions (Fig. 4B. 3A). The concentration of Fe decreases from base of the core to 44 cm from where it increases up to 8 cm before it maintains a decreasing trend towards the surface. Mn, Zn and Cu show increasing trend in the bottom 66 – 44 cm and then gradual increasing trend in the middle portion of 44 – 6 cm from where values decrease towards the surface. Cr shows a decreasing bottom portion of 66 – 52 cm and then an increasing trend in the middle portion of 52 – 28 cm from where it shows an erratic trend towards the surface. Co shows a more or less increasing trend from the base of the core towards the surface while Pb shows an erratic trend with ups and downs through out the core.

In case of core GN, the geochemical data shows a range of 3.77 - 8.43 % Fe, 204.25 -540.25 µg/g Mn, 37.50 - 118.50 µg/g Zn, 32.75 - 81.50 µg/g Cu, 105.75 - 191.25 µg/g Cr, 8 - 130 µg/g Co and 16.5 - 184.75 µg/g for Pb. All the metals except Pb agree with major elements and show three distinct portions with depth (Fig. 4B. 3B). The bottom portion 92 – 64 cm is characterized by plateau of enriched concentrations and decreasing trend which is followed by an increasing middle portion of 64 - 28 cm while the top portion of 28 cm to the surface is characterized by decrease in values. Pb shows overall an increasing trend from base of the core towards the surface.

Vertical distribution

A measure of the compositional variability of the inorganic component delivered to a marsh is revealed by the down core profiles of the elements that are constituents of detrital mineral phases and therefore unaffected by diagenesis [15]. The relative constancy of K/Al ratio with depth in both the cores is interpreted to imply that the composition of the accumulated material has not fluctuated dramatically over time. However, in core GH, there is slight change which may indicate change in input with change in grain size (Fig. 4B. 3A). No significant down core differences are observed in the X-ray diffraction spectra or in the clay mineral composition in the core GN (Fig. 5) and have therefore been derived from the same sediment source [16]. The identified clay mineral assemblage of kaolinite, chlorite, illite and smectite clearly reflects their derivation from the catchment area, which consists mainly of Precambrian crystalline rocks that are lateritised at places [17,18].

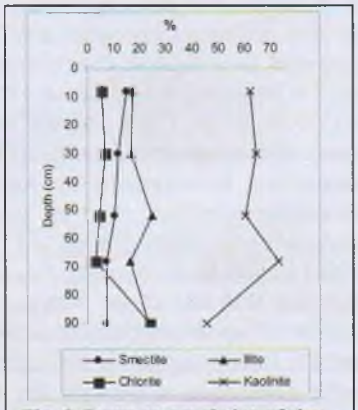

Fig. 5. Down core variation of clay minerals in core GN.

The diagenetic cycles of Fe and Mn are well known as they are dominant participants in bacterially driven aquatic redox processes [19] and presence of strong Fe and Mn peaks may indicate redox remobilization. So, the oxidized conditions, as indicated by Mn profile in core GH and Mn and Fe profiles in core GN, do persist from the surface to 6 cm in core GH and 28 cm in core GN. Any post-oxic zone, if present must be in between 6 to 44 cm and 28 to 64 cm in core GH and GN respectively where the Fe and Mn profiles show some enrichment with an overall decreasing trend but lack clear and consistent peaks. This may probably indicate that a stable redox zonation has not developed, as the area is frequently flooded and so will be subjected to a fluctuating water table. This will vary daily and monthly in response to land runoff as well as tide. A dynamic water table

will cause short term fluctuations in the redox boundary [20,21] which precludes the formation of sharp diagenetic Mn and Fe peaks [22]. The bases of the oxic - anoxic conditions in the cores are therefore inferred at 44 cm and 64 cm. The increase in Mn and Fe in the deeper zone in both the cores may demonstrate that they are trapped by authigenetic carbonate/sulfide formation where conditions are permanently reduced [23, 22]. The calcium profiles in both the cores support the above described diagenetic phenomenon. The sudden decline of Ca profile from surface over 6 cm to leave a tail of low value upto 44 cm in core GH and the decreased trend from surface to 68 cm in core GN are likely due to dissolution of $CaCO_3$ as acidity is generated in the pore waters of the oxic zones of the sediments [24]. Decalcification occurs in oxic salt marsh sediments in response to a lowering of pH resulting from nitrification and decomposition of organic matter [25,26]. The organic carbon profiles in both the cores agree with decreasing trends in the oxic-anoxic zones leaving enriched reducing zone in deeper portions of the cores. However, the deep increase in Ca concentration at deeper portion of core GH is likely due to authigenic carbonate formation in response to increase in pore-water alkalinity as sulfate is consumed and sulfides formed [22,27,28]. However, the vertical distributions of major elements especially Ca in core GH are also likely affected by variation in sediment source as indicated by K/Al ratio profile. The decrease of K/Al ratio from 54 cm down the core which is accompanied by sudden drop but still high value in organic carbon content with high Ca and Mg concentration may probably indicate a comparatively more marine input in addition to the diagenetic precipitation. The sudden rise of organic carbon content at 50 cm and upward decrease with sudden decrease of Ca and Mg may again signify the more terrigenous input which is modified by diagenesis.

The heavy metal profiles in core GH show similar distribution with depth demonstrating similarities in sources and/or post depositional behaviour. Heavy metals are normally scavenged from solution by fine sediments specially clay minerals and associated Fe, Mn and organic coatings [2,29]. However, heavy metals concentrations including Fe and Mn show poor association with Al (0.502, Fe; - 0.043, Mn; 0.191 Zn, -0.151, Cu; 0.530, Co; -0.048, Pb) and clay (0.354, Fe; 0.573, Mn; 0.253, Zn; 0.526, Cu; 0.163, Cr; 0.478, Co; -0.065, Pb) indicating that observed profiles are not a result of mineral variations [30]. The profiles are, therefore, presented in raw, rather than being normalized as suggested by Ackermann [31] and Grant and Middleton [32]. However, the distribution profiles may be partially due to early diagenetic processes [33] as well as environmental contamination [34]. Even though the profiles of heavy metals seem to be similar with Fe and Mn distribution, Fe and Mn show no significant correlation with heavy metals except with Cu. Still Mn shows better correlation than Fe signifying its role in redistribution of heavy metals. Mn shows significant correlation with Cu (0.749) and moderate correlation with Cr (0.422) and Co (0.462) while Fe maintains a moderate association with Cu (0.545) and Cr (0.441). The better association of Co with Mn than Fe reflects that Co is more cycled along with Mn oxides at redox boundaries [22]. The exclusive role played by Mn oxides in the cycling of Ni and Co has been reported earlier by Klinkhammer [35] and Shaw et al. [36]. Evidence of digenetic modifications can be seen with the peaks of Zn, Cu ,Cr and Co at depths 6 cm which coincides with Mn peak and peaks of Zn, Cu (28 and 40 cm) and Cr (28cm) with Fe and Mn, which indicate the coprecipitation with Fe and Mn oxides.

In core GN, Al shows significant correlation with clay (0.818), Fe (0.672), Mn (0.633) and moderate correlation with heavy metals (0.314, Cu; 0.463, Cr and 0.343, Co) and hence heavy metals including Fe and Mn are normalized with Al in order to remove the grain size effect. However, the bulk profiles are almost similar with normalized ones indicating minor mineralogical variations with depth. Fe shows a significant association with Zn (0.648), Cu (0.698) and moderate correlation with Cr (0.574) while Mn shows moderate association with Cr (0.418) and Co (0.332). The similarity in the profiles of Cu and Zn without pronounced peaks and their significant

association with Fe only suggests the distribution of Cu and Zn may be strongly controlled by Fe cycling than Mn cycling in this core. Allen et al. [37] identified a similar pattern for Cu, Pb and Zn in sediments from the Severn estuary. On the other hand, Mn shows moderate association with coincident pronounced peaks with Cr (4, 36, 42, 56 cm) and Co (4, 22, 36 cm) reflecting that they are more cycled along with Mn oxides [22]. There is evidence for coprecipitation of all heavy metals with Fe and Mn oxyhydroxides as they show enrichment in the lower permanently reduced zone. So, in the oxidizing and partially reducing middle zone, they exhibit readsorption with Fe/Mn oxyhydroxides, and following early diagenetic movement of trace metals in the surface oxic layer and in the highly reducing lower layers [22]. However, the gradually increasing Pb profile towards the recent strata, which is totally in contrast with redox sensitive Fe and Mn profile, may suggest an anthropogenic source.

Spatial distribution

The sediment characteristics and geochemistry of the two cores described above indicate considerable variations between them. The core GH is of mature mudflat and consists of slightly sandy mud whereas core GN is characterized by comparatively coarser sediments of sandy mud of a mudflat environment. The difference in sediment characteristics may be due to the varying distances from the source. A simple yet effective way of showing the variations between sites is by using isocon diagrams [3,38]. These plots compare the average values of specific components from different sites.

The isocon diagram (Fig. 6) indicates that there is little difference in Al, K, Fe, Zn, Cu and Cr concentrations between the two cores. There are, however, significant differences in sediment components and more importantly in concentrations of Ca, Mg, Pb and Co. Core GH shows high concentrations of Ca, Mg, and Cr together with high percentage of silt, clay and organic carbon. The high concentrations of Ca and Mg are likely due to marine influence in this mudflat which is relatively nearer to sea while high organic carbon, Mg, to some extent Cr and Fe, may be caused by grain size effect. On the other hand, core GN shows relatively higher concentrations of Pb and Co together with higher value of sand. The higher values of sand and high concentrations of Pb and to some extent Co are likely to be caused due to its proximity to continental source reflecting a pollution origin.

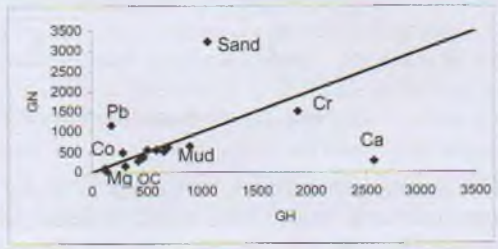

Fig. 6. Isocon diagram. Individual points represent average value of sediment component and element in each core. To ensure all elements plot on the same scale, major elements (%): Al, K, Mg, Fe, sand, and OC are multiplied by 100; Ca and Mn (μg/g), by 1; Zn, Cu, Cr, Co, Pb, silt, and clay by 10.

Sedimentation rate and Enrichment Factor

The profiles $^{210}Pb_{excess}$ are presented in figure 7. In case of core GH, there is a relatively log-linear decrease of $^{210}Pb_{excess}$ activity with depth but with a change in slope at 26 cm depth (Fig. 7A). Changing slope in the $^{210}Pb_{excess}$ profile indicates variation in accumulation rate or is due to bioturbation [2]. The assumption of closed system might be violated in salt marshes due to early diagenetic remobilization of ^{210}Pb [39,40]. In the present study, there is no obvious change in the shape of $^{210}Pb_{excess}$ profile in the vicinity of the oxidized/reduced boundary, as would be expected if ^{210}Pb migration had taken place. When the profiles of ^{210}Pb are compared with Pb and redox

sensitive elements, there are no similar peak concentrations negating the possibilities of mobilization of ^{210}Pb. The higher values of ^{210}Pb in top 26 cm do not coincide with the proposed oxidized/partially reducing boundary and not even with partially reducing/reducing boundary. However, the concentration minima occur below 35 cm, which are taken as background values, may highlight the possibility of diagenetic movement as 32 cm depth is the transition of colors recorded in field, but is apparently not significant enough to explain the change in slope at 26 cm depth. Therefore, the change in slope at 26 cm strongly suggests change in sedimentation as also supported by the K/Al ratio profile and not due to bioturbation. Hence the sedimentation was slower at 0.16cm/yr until 26 cm, which corresponds to the year 1982 and increased thereafter to 2 cm/year.

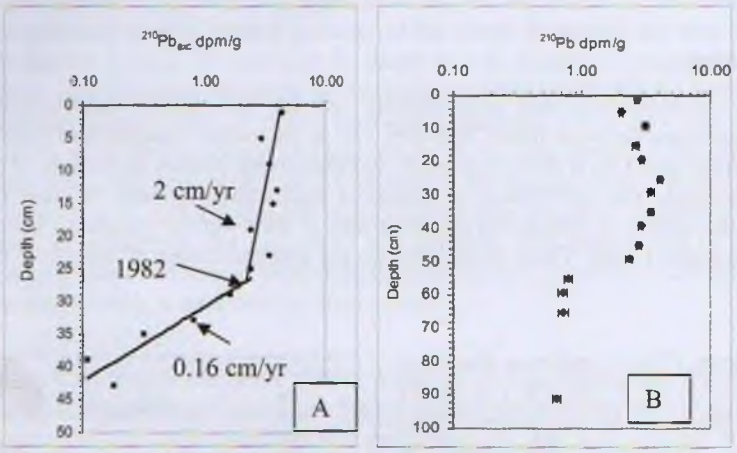

Fig. 7. Down core profiles of 210Pb: A – core GH, B - core GN.

To evaluate anthropogenic influences of heavy metals in sediments, enrichment factor (EF) has been used as an index. It is a useful indicator reflecting the status of environmental contamination. In core GH (Fig. 8A), the EF values of Mn and Zn are below 1 except at some points while Pb values are less than 1.5 with higher values at some points suggesting that these metals may be entirely from crustal materials or natural weathering processes [10]. On the other hand, EF values of Fe, Cr and almost all the values of Co are higher than 1.5 which suggest that a significant portion of these metals are delivered from non-crustal materials, or non-natural weathering processes. Throughout the core, EF values of Fe is more than 1.5 which is gradually increasing upwards with the values more than 2 from 22 cm upwards corresponding to the period from 1994 to present. EF values of Cu are below 1.5 up to 22 cm which corresponds to the year 1994 from where it increases to present. Co starts enrichment (>1.5) from 48 cm which corresponds to the year 1904 to present day with a marked increase from 1994 onwards. Cr is the most enriched metal in the core with values greater than 2 throughout the core. So, the EF of the present study shows environmental contamination by Fe, Cu, Cr and Co in recent years especially from 1994.

In case of core GN, the total ^{210}Pb profile does not show decay with depth (Fig. 7B). It shows some pattern in the top portion of 0 – 50 cm in which all the values are more or less same representing a zone of sediment mixing. Then the values suddenly drop below 1 (0.64 – 0.79 dpm/g) from 54 cm to the base of the core leaving a gap from 50 to 54 cm. This gap of depletion is probably caused by erosion or removal of sediments by human activities leaving mixed sediments. So, sedimentation rate of this core could not be calculated.

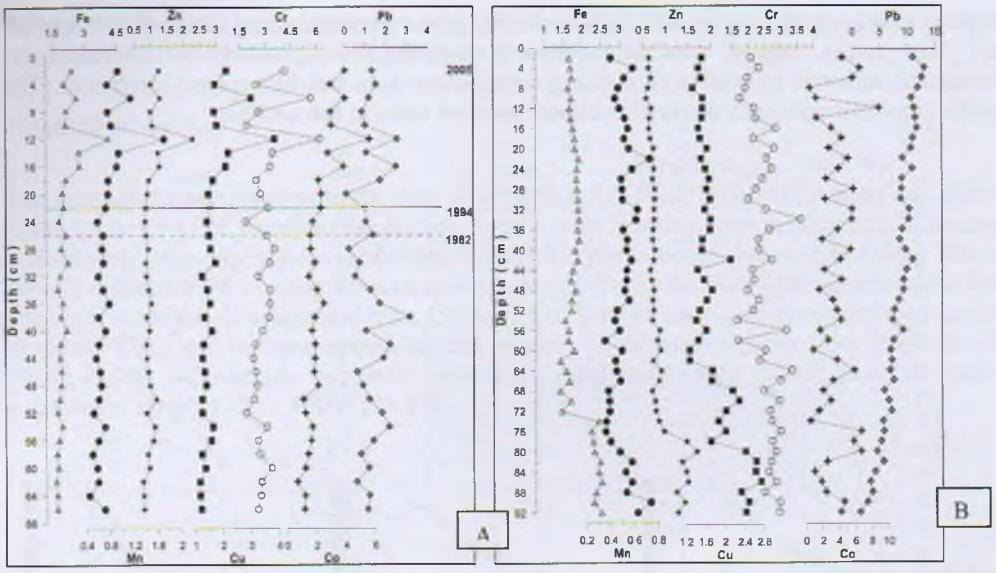

Fig. 8. Down core trends of metal enrichment factors (EF): A – core GH, B – core GN.

The EF values of all the metals except Pb show more or less similar trend throughout the core except the down portion (< 68 cm) in which, interestingly, all the metals are enriched (Fig. 8B). As explained above, the enrichment of metals is probably caused by the diagenetic processes in the permanently reducing zone. So, the construction of pollution chronology in this core is limited by different processes. However, in the top portion, EF values Mn and Cu are less than 1 while the values of Fe and Cu are below 2. On the other hand, Cr and Co are highly enriched with values above 2. Pb, unlike in core GH, shows gradually increasing trend towards the surface with enrichment values above 5 which may signify higher degree of contamination nearer to land.

Magnetic susceptibility

The rock magnetic parameters are shown in figure 9. Common features are observed in the rock magnetic parameters between the two cores. In both the cores, the concentration dependent magnetic parameters (χ, χ_{ARM} and SIRM); magnetic mineralogy related parameters (S_{300} in core GH and HIRM) and grain size indicators (χ_{ARM}/χ and χ_{ARM}/SIRM) have relatively high values in the middle and upper portion of the cores. The values show down core drop in the middle portion before maintaining an almost constant trend in the bottom portions of the respective cores. So, one can divide the entire core into three sections according to variations of the magnetic parameters.

In core GH (Fig. 9A), Section 1 (66 – 50 cm) has low values for all the parameters. The values of χ, χ_{ARM}, HIRM and grain size index ratios have almost constant trend whereas SIRM and S_{300} show slight enrichment towards the bottom of the core. In section 2 (50 – 42 cm), all the parameters undergo a sudden increase especially in the upper 4 – 6 cm of this section and drop to their minimum values at ~50 cm. S_{300} value increases sharply from 0.65 at about 50 cm depth to 0.75 at the top of this section. These changes indicate that the dominant magnetic minerals rapidly change up the core from high-coercivity components to low-coercivity minerals. HIRM values too, progressively increase up the core indicating that the partial increase of high-coercivity minerals

took place in this section. In section 3 (42 – 0 cm), all the parameters are enriched with highest values. S_{300} values suggest that this section is magnetically dominated by low-coercivity ferromagnetic minerals together with a strong contribution from anti-ferromagnetic minerals. The magnetic granulometric index displays an almost constant value in this section.

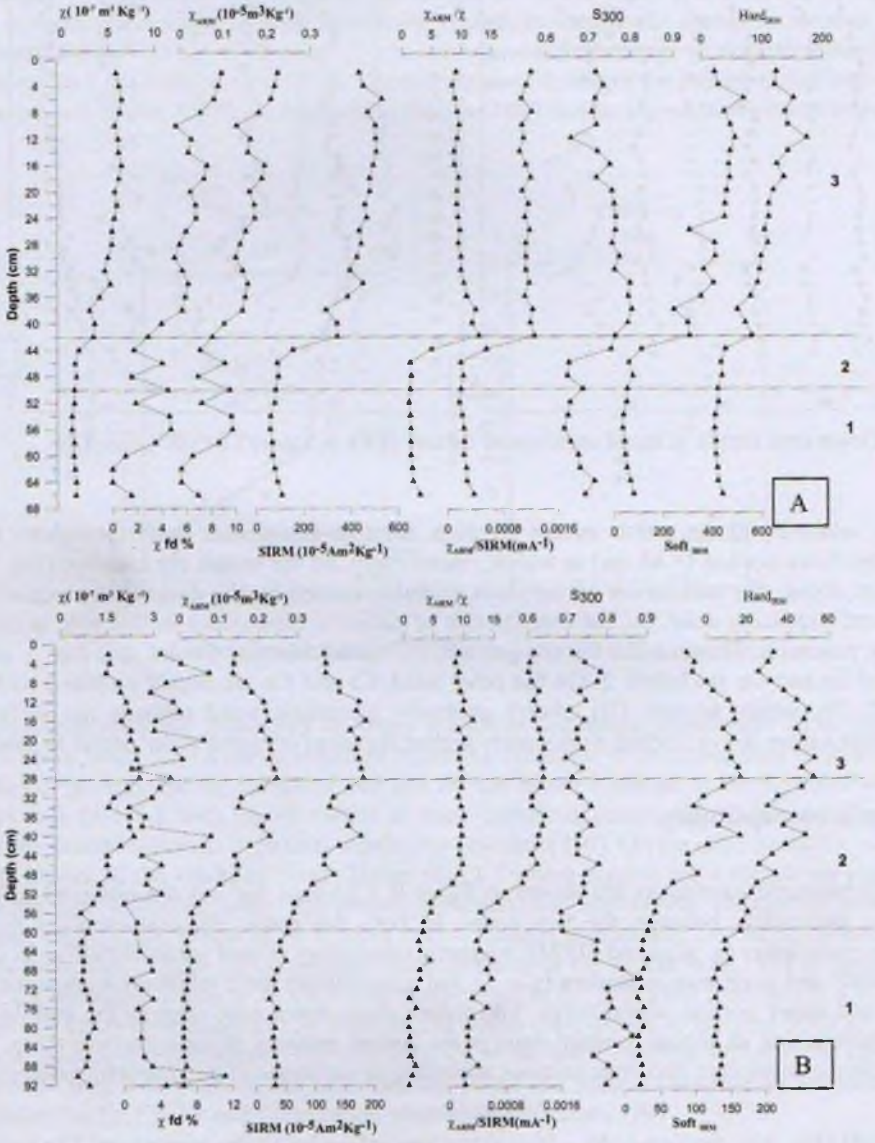

Fig. 9. Magnetic profiles: A – core GH, B – core GN.

In core GN, the profiles of concentration dependent parameters (χ, χ_{ARM}, and SIRM) and HIRM (Fig. 9B) agree with the geochemical profiles in all the three sections. In the bottom section 1 (92 – 60 cm), all the parameters except S_{300} show a more or less constant trend. S_{300} value maintains a high value and a nearly constant trend before it decreases in the upper portion of this section. In the second section (60 – 28 cm) all the parameters are gradually increasing upwards and display highest

value at 28 cm depth. In the last section 28 -0 cm, the values of concentration dependent parameters (χ, χ_{ARM}, SIRM) and HIRM gradually decrease towards the surface.

Magnetic mineralogy

The thermal demagnetization curves for selected samples from different sections are shown in figure 10. In core GH, samples from section 3 and 2 show similar curves in which the IRM undergo a monotonic decay until their unblocking at ~680^{0}C, which is indicative of hematite. The most distinct difference for samples from section 1, compared to those from higher parts of the core is that there is considerable decrease from 150 to 350^{0}C. Gregite has higher coercivity than magnetite (Roberts, 1995) and is characterized by loss of most of its magnetization from 200^{0}C to 350^{0}C [41,42,43,44]. In contrast, pyrrhotite undergoes rapid unblocking within a much narrower temperature range of 320 – 350^{0}C [44,45].

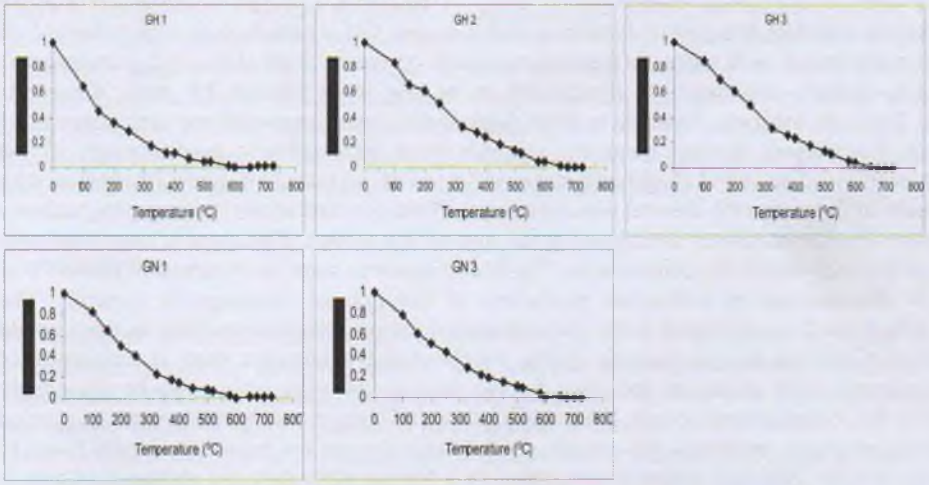

Fig. 10. Representative thermal demagnetization curves for different sections in cores GH and GN.

There is a possibility that the loss in magnetization at around 200 - 320^{0}C is due to maghemite or titanomagnetite. But the slight increase in the magnetic susceptibility at around 300^{0}C in χ(T) curve may attribute the presence of gregite (Fig. 11). Finally, the values are unblocked to near zero at about 580^{0}C, which suggests that magnetite is also present and there is little hematite in this section. On the other hand, in core GN, samples from all sections (section 1 and 3 are represented) show similar curves in which the IRM undergo a monotonic decay until their unblocking at ~580^{0}C, which is indicative of magnetite. So, it can be concluded that in core GH, the magnetic properties of section 3 and 2 contain substantial contributions from hematite as well as magnetite. In contrast, the magnetic mineralogy of section 1 is characterized by (titano)magnetite and gregite, with little hematite. However, core GN shows the uniform mineralogy throughout the core, which is characterized by magnetite with little hematite.

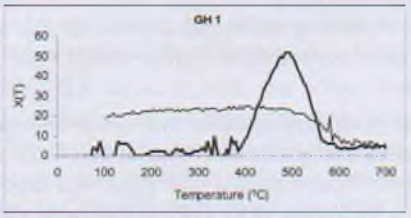

Fig. 11. Representative curve of temperature dependence of magnetic susceptibility

The magnetic parameters are extremely sensitive and small changes in catchment area processes would be recorded in the sediments. It is clear from the correlation that there is no significant relationship between SIRM with Al (-0.49), Mg (-0.44) and K (0.07) in core GH indicating little supporting evidence of catchment area changes (Mackereth, 1966). However, changes in the catchment area processes can be the explanation for core GN as SIRM shows moderate correlation with Al (0.54), Mg (0.54) and K (0.75). The data suggest that there has been a fining upwards of the magnetic grain size as well as increase in total concentration. This pattern is consistent with the suggestion that fine grains have been dissolved and the multi domain grains broken up into Stable Single Domain (SSD) grains. The finer component is believed to be dissolved first due to its high surface to volume ratio, which would result in a reduction in magnetic intensity as well as a shift in grain size towards the coarse end [46,47]. Hence the precipitous down core drop of magnetic parameters from 42 cm and 28 cm in core GH and GN respectively, which is diagnostic of early diagenesis in deep water marine sediments[46,48] and may reflect the onset of reducing condition.

The section 3 in core GH and part of sections 3 and 2 in core GN are marked by high values of all concentration dependent bulk magnetic parameters, nearly constant values of S_{300} and granulometric index. These sections are therefore interpreted to be the least affected by early diagenesis influences. The main magnetic minerals in these parts of the cores (magnetite and hematite) can be regarded as the primary detrital magnetic minerals prior to diagenetic modifications in the underlying sections. The initial diagenetic stage, observed in section 2 of core GH, begins with sharp increase in ferrimagnetic mineral concentrations. These concentrations increase progressively upwards from absolute minimum abundance at the start of this section. This stage is associated with depletion of the high-coercivity components. The later diagenetic stage as observed in section 1 of core GH is characterized by authigenic production of fine-grained ferrimagnetic minerals. The section 1, which has been subjected to the initial diagenetic stages like the overlying sections would have retained, if any, the largest magnetic grains. On the contrary, however, there is enrichment of Superparamagnetic (SP) grains as indicated by the increase of $\chi_{fd}\%$ which can be reasonably interpreted to be of authigenetic origin. Thermomagnetic and temperature measurements suggested the possibility of gregite present in this section. Sedimentary gregite has been consistently found to have Single Domain (SD) like magnetic properties [49]. On the other side, the section 1 of core is characterized by slight increase in χ and sudden increase in S_{300} which also suggests the possibility of authigenetic origin. However, the similarity in monotonic decrease of thermal magnetization curve in different sections limited the explanation of possible gregite present in this section. The sudden increase in organic carbon content and ferromagnetic minerals together with high sand content may suggest the possibility of more terrigenous input during this time before it was subjected to diagenetic modifications in later stage.

It has been demonstrated that environmental magnetism can be used as a proxy indicator of heavy metal concentration in a simple, quick and non-destructive way [50,51]. The considerable similarity between heavy metals and χ_{ARM} was reported from intertidal sediments of the Yangtze Estuary, China by Zhang et al. [52]. It has been suggested that certain magnetic parameters can be used as grain size proxy [53,54]. Zhang et al. [54] reported strong relationship between χ_{ARM} and to a lesser degree, frequency dependent susceptibility (χ_{fd}) with heavy metals and explained the role of particle size effects and iron oxides in controlling metal concentration. However, in the present study, even though χ_{ARM} in GH and both χ_{ARM} and χ_{fd} in GN show good correlation ($r > 0.5$) with clay, they show poor correlation ($r < 0.5$) with the metals studied except Co in GH; Mn and Pb in GN. Therefore, the changes in the heavy metal concentrations in this core cannot be accounted for by particle size alone. Hence, it is likely that the reduction of iron oxide plays a significant role in distribution of heavy metals. However, the change in magnetic properties in section 3 of both the cores, which are considered as the primary detrital minerals, point to both quantitative and

qualitative changes in the assemblage of magnetic minerals present. The increase in SIRM reflects an increase in total magnetic mineral concentrations. In combination with SIRM, the increase of the hardest remanence component points to an increase in hematite in both relative and absolute terms. The trend in 'soft' and 'hard' isothermal remanence can be plotted on a mass specific basis and this isolates these two properties from all other variables responsible for changes. In the present study, it confirms that both components increase significantly in the upper levels of cores which are diagenitically least affected. The constant nature of grain size parameters in these sections indicate a nearly uniform grain size and hence suggest a similar condition of deposition with negligible post depositional modifications. When the calculated 'soft' i.e. mostly magnetite, 'hard' i.e. mostly hematite, and total i.e. SIRM trends were compared, there were interesting parallels and differences. The increase is much steeper in hematite to magnetite suggesting the relative higher deposition of hematite in recent years.

There is link between magnetic properties (χ, χ_{fd}, χ_{ARM} and SIRM) and metals (Fe, Mn, Zn, Cu and Co) in the upper section of the cores wherein the rate of sedimentation recorded is very high. Most importantly, there is parallelism in trends of 'hard' and 'soft' profiles with metals, which points to a possible common origin. Gradual increase in χ_{fd} value towards the surface along with metals is likely because of relative higher degree of weathering and erosion in recent years. This may reflect trace metal enrichment of the magnetically enhanced soil derived clays during weathering and transport in recent years with enhanced sedimentation rate especially in core GH.

Conclusions

The mudflats of Tadri estuarine system show vertical as well as spatial variation in sediment components and metals along the estuary. The core GH is of mature mudflat consisted of slightly sandy mud with higher concentrations of Ca, Mg and Mn together with higher silt, clay and OC percentage, which is likely because of more marine influences in this mudflat and by grain size effect whereas core GN is characterized by comparatively coarser sediments of sandy mud of a mudflat environment and shows higher concentrations of Pb and Co together with higher value of sand, which are likely to be caused by comparatively nearer to continental source reflecting a pollution origin. The clay mineralogy suggested little changes in source or provenance over the observed sedimentation period. The unsupported ^{210}Pb activity in core GH two phases of sedimentation, a relatively low to higher rate of sedimentation with time. The geochemical data indicates that both Mn and Fe have been remobilized and that these diagenetic processes have slightly modified the vertical distributions of Zn, Cu, Cr and Co. The magnetic data reveal evidence for changes in magnetic mineralogy and grain size within the cores. In both the cores, there is substantial decrease in total magnetic concentration and coarsening of the magnetic grain size, but at different depths, which is in agreement with Fe and Mn profiles, suggesting dissolution of fine grained magnetite under reducing conditions. However, general trends in pollutant loading, as indicated by EF of Cu, Cr, Co and Fe can still be identified in Core GH with maximum inputs (EF > 1.5) occurring around 1900 increasing towards the present day. Both cores show closely similar traces of gradual increase of hematite and magnetite deposition with a steeper rise of hematite in the upper part of the respective cores which may reflect the increased erosion of more weathered (magnetically harder) materials with increase in anthropogenic activities. Though, the construction of pollution chronology in the core GN is limited by different processes, unlike in core GH, Pb shows gradually increasing trend towards the surface with enrichment values above 5 which may signify input of higher degree of contamination upstream side of the estuary.

References

[1] N. J. Valette- Silver: Estuari., V. 16 (1993), p. 577 - 588.
[2] A.B. Cundy and I.W. Croudace: J. Environ. Radioact., V. 29 (1995), p. 191–212.
[3] A.B. Cundy, I.W. Croudace, J. Thomson and J. T. Lewis: Environ. Sci. Technol., V. 31 (1997), p. 1093-1101.
[4] R. L. Folk: *Petrology of Sedimentary rocks.* (Hemphills. Austin, 1968).
[5] H. E. Gaudette, W. R. Flight, L. Toner and D. W. Folger: J. Sedi. Petro., V. 44 (1974), p. 249 - 253.
[6] P. E. Biscaye: Geol. Soc. Amer. Bull., V. 76 (1965), p. 803 – 832.
[7] F. Oldfield: J. Paleolimnol., V. 4 (1990), p. 93 - 101.
[8] R. Thompson and F. Oldfield: *Environmental Magnetism* (Allen and Unwin, London 1986).
[9] J. A. Grant: Econ. Geol., V. 81 (1986), p. 1976 – 1982.
[10] J. Zhang and C.L. Liu: Coast. Shelf Sci., V. 54 (2002), p. 1051 – 1070.
[11] K.K. Turekian and K. H. Weedepohl : Bull. Geol. Soc. Amer., V. 72 (1961), p. 175 - 192.
[12] H. E. Reineck and W. Siefert: Die Kuste, V. 35 (1980), p. 26 – 51.
[13] B. W. Flemming: Cont. Shelf Res., V. 20 (2000), p. 1125 – 1137.
[14] M. Pejrup: *Tide – influenced sedimentary environments and facies. Reidel, Dordrech* (1988), p. 289 – 300.
[15] J. R. L. Allen: Sedi. Geol., V. 53 (1987), p. 73 – 100.
[16] K. L. Spencer, A. B. Cundy and I. W. Croudace: Estuar., Coast. Shelf Sci., V. 57 (2003), p. 43 – 54.
[17] H. Chamley : *Clay sedimentology* (Springer, Berlin Heidelberg New York 1989)
[18] V. P. Rao and B. R. Rao: Cont. Shelf Res., V. 15 (1995), p. 1757 – 1771.
[19] W. Stumm and J. J. Morgan: *Aquatic Chemistry* (Wiley, New York, NY, 2nd ed. 1981)
[20] W. H. Casey and A. C. Lasaga: Geochim. Cosmochim. Acta, V. 51 (1987), p. 1109 – 1120.
[21] M.E. Hines, S.L. Knollmeyr and J.B. Tugel: Limnol. Oceano. V. 34 (1989), p. 578 – 590.
[22] J. J. G. Zwolsman, G. W. Berger and G. T. M. Van Eck: Mar. Chem., V. 44 (1993), p. 73 – 94.
[23] R. Mc Caffrey and J. Thomson: Adv. Geophys., V. 22 (1980), p. 165 – 236.
[24] P. N. Froelich, G. P. Klinkhammer, M. L. Bender, N.A. Luedke, G. R. Heath, D. Cullen and P. Dauphin: Geochim. Cosmochim. Acta, V. 50 (1979), p. 1075 – 1090.
[25] G.W. Luther and T. M. Church: Mar. Chem., V. 23 (1988), p. 295 – 309.
[26] M. Vranken, O. Ocnema and J. Mulder: Hydrobiol., V. 195 (1990), p. 13 – 20.
[27] J. F. Gaillard, H. Pauwels and G. Michard: Oceanol. Acta, V. 12 (1989), p. 175 – 187.
[28] K. Pye, M. L. Coleman and W. M. Duan: *Biogeochemistry of intertidal Sediments.* (Cambridge University Press, 1997, p. 119 – 151).
[29] L. Bendell – Young and H. H. Harvey: Limnol. Oceanogr. V. 37 (1992), p. 603 – 613.
[30] A. Cearreta, M. J. Irabien, E. Leorri, I. Yusta, I. W. Croudace and A.B. Cundy:. Estuar., Coast. Shelf Sci., V. 50 (2000), p. 571 – 592.
[31] F. Ackermann: Environ. Technol. Lett., V. 1(1980), p. 518 – 527.
[32] S. H. Grant and R. Middleton: Estuar., Coast. Shelf Sci., V. 31(1990), p. 71 – 85.
[33] R. A. Berner: *Early Diagenesis: a Theoretical Approach* (Princeton University Press, Princeton, N.J., 1980, pp. 241).
[34] D. H. M. Anderton: *Historical Monitoring. Monitoring and Assessment Research Centre* (University of London, 1985, p. 1 – 95).
[35] G. P. Klinkhammer: Earth Planet. Sci. Lett., V. 49 (1980), p. 81 – 101.
[36] T. J. Shaw, J. M. Gieskes and R. A. Jalinke: Geochim. Cosmochim. Acta, V. 54 (1990), p. 1233 – 1246.

[37] J. R. L. Allen, J. E. Rae and P. E. Zanin: Mar. Pollut. Bull., V. 21 (1990), p. 574 – 580.
[38] J. A. Grant: Econ. Geol., V. 81(1986), p. 1976 – 1982.
[39] J. R. L. Allen, J. E. Rae, C. Longworth, S.E. Hasler and M. Ivanonovich: Estuar., V. 16 (1993), p. 670 – 677.
[40] A. B. Cundy: *Radionuclide and geochemical studies of recent sediments from the Solent estuarine system (*Ph. D. thesis. Univ. Southampton, Southampton, UK, 1994)
[41] M. Krs, M. Krsova, L. Koulıkova, P. Pruner and F. Valın: Phys. Earth Planet. Inter., V. 70 (1992), p. 178– 186.
[42] R. L. Reynolds, M. L. Tuttle, C. A. Rice, N. S. Fishman, J. A. Karachewski, and D. M. Sherman: Amer. J. Sci., V. 294 (1994), p. 485 – 528.
[43] A.P. Roberts: Earth Planet. Sci. Lett., V. 134 (1995), p. 227-236.
[44] M. Torii, K. Fukuma, C. S. Horng and. T. Q. Lee: Geophys. Res. Lett., V. 23 (1996), p. 1813 – 1816.
[45] M. J. Dekkers, H. F. Passier and M. A. A. Schoonen: Geophys. J. Int., V. 141(2000), p. 809 – 819.
[46] R. Karlim and S. Levi: Nature, V. 303 (1983), p. 327 - 330.
[47] J. J. Bloemendal, J. W. King, A. Hunt, P. B. DeMenocal and A. Hayashida: J. Geophys.Res., V. 98 (1993), p. 4199 – 4219.
[48] S. G. Robinson, J. T. S. Sahota and F. Oldfield: Mar. Geol., V. 163 (2000), p. 77 – 107.
[49] I. F. Snowball: Phys. Earth Planet. Inter., V. 68 (1991), p. 32 – 40.
[50] M. Scoullos, F. Oldfield and R. Thompson: Mar. Pollut. Bull., V. 10 (1979), p. 287 – 291.
[51] A. Berry and A. J. Plater: Water, Air Soil Pollut., V. 106 (3 – 4) (1998), p. 463 – 479.
[52] W. Zhang, L. Yu and S. M. Hutchinson: Sci. Total environ., V. 266 (2001), p. 169 – 175.
[53] F. Oldfield and L. Yu: Sedimentol., V. 41(1994), p. 1093 - 1108.
[54] W. Zhang, L. Yu, M. Lu, S. M. Hutchinson and H. Feng: Environ. Pollut., V. 147 (2007), p. 238 – 244.